

Simultaneous Measurements of Gas-Solid Flow Rates and Pressure Drop in Downcomer of J-Valve in CFB

T. Goshima and K. Terasaka^{*,†}

School of Science for Open and Environmental Systems,
Graduate School of Keio University, 3-14-1, Hiyoshi, Kohoku-ku,
Yokohama 223-8522, Japan; moonrose7302000@a5.keio.jp

^{*}Department of Applied Chemistry, Keio University, 3-14-1, Hiyoshi,
Kohoku-ku, Yokohama 223-8522, Japan; terasaka@applc.keio.ac.jp

Original scientific paper
Received: May 21, 2007
Accepted: October 12, 2007

To monitor the gas and solid streams in a downcomer of a J-valve in a CFB, the simultaneous measurement technique using the oxygen gas tracer, the hot particle tracer and the pressure drop was developed. By using this novel measurement technique, the dependence of the solid flow on the gas flow in the moving bed in the downcomer of J-valve was investigated. The pressure profile and the pressure balance in the J-valve as well as the CFB were measured. It was clarified that the circulating mass flux in a CFB or solid flow in a J-valve was governed by the pressure drop in the downcomer of the J-valve.

The pressure drop in the downcomer of the J-valve was well estimated using the modified Ergun's equation. To quantitatively control the circulating rate of the solid particles in the CFB, the monitor and tuning of the superficial gas velocity in the downcomer of the J-valve was important.

Key words:

Flow measurement, tracer method, pressure drop, J-valve, circulating fluidized bed

Introduction

Circulating fluidized beds (CFBs) are commercially used in many kinds of gas-solid contacting processes, such as the FCC process, Synthol process and coal combustor, because they have several advantages, such as low erosion, excellent phase contact, well-controlled temperature profile and easy scale-up. The papers in terms of the CFB have been surveyed by Van de Velden *et al.*,¹ Lei and Horio,² Kim *et al.*,³ Rhodes and Geldart,⁴ Basu and Cheng,⁵ Smolders and Baeyens,⁶ Gupta and Berruti,⁷ Horio and Mori⁸ and Mori *et al.*⁹

To efficiently operate CFB, it is important to smoothly circulate the solid particles through every part of the CFB. When the CFB is utilized as a chemical catalytic reactor, the control of the circulation rate of the catalyst is critical because it governs the reaction rate in the system. Oshima *et al.*¹⁰ and Wachi *et al.*¹¹ applied the CFB catalytic reactor with a J-valve for a dichloroethane production process. In their system, two kinds of catalytic chemical reactions steadily occur in two fluidized bed reaction columns, between which the catalytic particles have to smoothly circulate. Although there are also mechanical feeders such as a screw, rotary, butterfly and slide valves to control the solids flow

rate, the pneumatic feeders have more advantages than the mechanical ones. The J-valve, L-valve, V-valve and loop-seal as typical pneumatic feeders have no moving parts so that they hardly cause trouble and they can be operated even at high temperature.^{12,13}

There are several papers describing the design of the pneumatic feeders: Kunii and Levenspiel¹⁴ summarized a number of articles in terms of particle flow in vertical and horizontal pipes as pneumatic valves. Geldart and Jones¹⁵ proposed correlations relating the aeration gas and the pressure drop across the L-valve to the solids flux. Yang and Knowlton¹⁶ visualized the L-valve and correlated the solid flow rate, aeration rate and pressure drop across the L-valve. Kim *et al.*¹⁷ developed a loop-seal with a downward tangential aeration system to provide higher solid circulation rates in the CFB in order to use weak particles.

For some gaseous catalytic reaction systems,^{10,11} the reactant gas flow rate has to be controlled independently of the catalytic particle flow rate. It is well known that the J-valve and loop-seal can possibly do this due to their unique geometry. Terasaka *et al.*¹⁸ investigated the gas and solid flow rates as well as pressure drop throughout a J-valve which was isolated from the CFB. They reported that the particle flow rate can be related using the modified

[†]Corresponding author

Ergun's equation to the gas flow rate in the J-valve. For industrial use, however, the solid particles out of the J-valve are recycled to the entrance of the J-valve. Moreover, it is unknown how the pressure balance in the CFB affects the pressure profile in the J-valve. There are few studies on the gas-solid flow rates and pressure profile in the CFB because of their very complex behavior.

To evaluate the gas-solid behavior in the CFBs, the tracer techniques have been sometimes employed. When the tracer technique is utilized, it is important to choose a tracer material and to consider an introducer and a detector.

There are a variety of tracers for gas and solid systems.¹⁹ Smolders and Baeyens²⁰ measured the solids' residence time distribution using a salt tracer using an electrical conductivity meter. Bhusarapu et al.²¹ investigated the mixing of solids in a gas-solid riser by a single radioactive tracer particle tracking. Gayan *et al.*²² used a CO₂ gas tracer to evaluate the radial dispersion in the CFB-riser and indicated that the gas stream in the dilute phase region is assumed to be plug flow. Li *et al.*²³ estimated the entrained gas flow rate in the downcomer of a CFB reactor with a V-valve using a H₂ gas tracer. Terasaka et al.¹⁸ measured only the entrained gas flow rate through a J-valve using a CO₂ gas tracer. The solid flow rate was calculated by the discharged solid weight out of the J-valve using an electronic balance.

For the paper reviewed above, there is no literature on the simultaneous measurements of the gas flow rate and solid flow rate by the tracer techniques directly injected into a J-valve.

In this study, therefore, a unique technique was developed to simultaneously measure the gas flow rate, the solid flow rate and the pressure drop in a J-valve mounted in a CFB. The observed gas-solid flow rates and the pressure drop observed by this simultaneous measuring technique were theoretically related to the design of the J-valve.

Experimental

Physical properties of solid particle

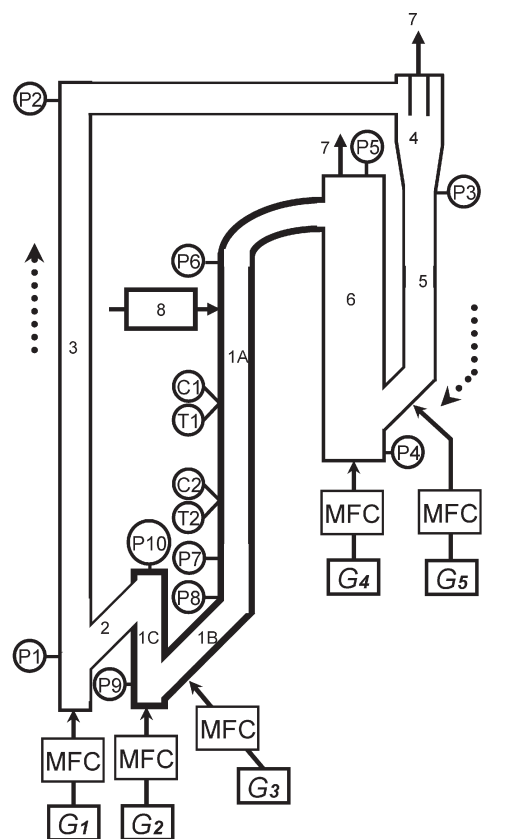
As typical fluidized particles for industrial catalytic reactors, γ -alumina particles are very often used due to their low cost, large specific area and thermochemical stability. In this study, therefore, porous γ -alumina powder (Mizusawa Kagaku Kogyo Co., Ltd.: Neobead MSC-1A) was used as the fluidized solid particles, which were classified as Geldart's group A'. Table 1 shows the physical properties of the fluidized particles used in this study.

Table 1 – Physical properties of fluidized particle

| | |
|---|-------|
| Particle density ρ_s [kg/m ³] | 1369 |
| Fractional voidage in particle ε_s [–] | 0.555 |
| Fractional voidage in bed at minimum fluidization velocity ε_{MF} [–] | 0.439 |
| Mean particle diameter d_p [μ m] | 43.4 |
| Standard deviation of diameter σ [μ m] | 13.6 |
| Repose angle θ [deg] | 30 |
| Minimum fluidization velocity U_{MF} [mm/s] | 1.53 |
| Sphericity ϕ [–] | ca.1 |

J-valve and operation

Figure 1 shows a J-valve in the CFB system. The J-valve was made of transparent acrylic resin as was the CFB. The solid particles were fed from the reservoir to the entrance of the J-valve. The solids out of the exit of the J-valve were fed to the



1 J-valve (A: Downcomer, B: Connector, C: Riser)
 2 Feeder
 3 Fast fluidized bed
 4 Cyclone
 5 Dipleg
 6 Reservoir
 7 Vent
 8 Tracer injection system
 (P) Pressure port
 (C) O₂ sensor
 (T) Thermometer
 (G) Gas flow rate

Fig. 1 – Experimental setup of J-valve and CFB

feeder, then they were recycled to the reservoir via the fast fluidized bed, the cyclone and the dipleg. The J-valve was divided into three parts, i.e., the downcomer, connector and riser corresponding to (1A) to (1C) in Fig. 1. The length of the downcomer, L_D , is 1.00 m. The connector's length, L_C , is 300 mm. The riser's height, L_R , is 270 mm. The dimensions of the other primary parts are as follows: The feeder's length, L_{inj} , is 380 mm. The inner diameter of the CFB except for the reservoir, the cyclone and J-valve was a uniform 24 mm. The height of the fast fluidized bed L_1 was 2.29 m. The height of the reservoir whose inner diameter was 100 mm, L_2 , was 490 mm. For the solid particles to smoothly flow, the dipleg, the connector and the feeder were inclined 45 degrees which was greater than the repose angle θ .

Dry air was used as the fluidized gas. The five aeration gas flow rates, G_1 to G_5 , were controlled using five mass flow controllers (MFC) as shown in Figure 1. The aeration gas flow rates of the fast fluidized bed, J-valve riser, reservoir and dipleg, G_2 , G_4 and G_5 , were fixed at constant values. The fluidized gas flow rate into the fast fluidized bed, G_1 , was maintained at 40 liters/min, i.e., superficial velocity = 1.47 m/s, that was greater than the transport velocity = 1.20 m/s. The fluidized gas flow rate into the rise of the J-valve, G_2 , was maintained at 2.76 mm/s greater than the minimum fluidized velocity so that the bed in the J-valve's riser was well fluidized and smoothly moved into the feeder. The fluidized gas flow rate into the reservoir, G_4 , was maintained at the minimum fluidization velocity so that the bed in the reservoir was fluidized and the bed height remained constant. The fluidized gas flow rate into the dipleg, G_5 , was as low as possible to prevent bridging in the dipleg.

The fluidized gas flow rate into the J-valve's connector, G_3 , was very important for controlling the particle flow rate through the J-valve so that its superficial gas velocity was changed within the range of 1.40 to 2.76 mm/s.

The effluent gas was exhausted from the vents at the top of the cyclone and the top of the reservoir.

The solid mass flux, F , was changed within the range of 2.41 to 9.93 kg/m²s in which the fluidization condition in the downcomer was kept in a homogeneous regime.

Measurement of gas stream in downcomer of J-valve

To observe the air stream through the J-valve, the gas tracer technique was used. Pure oxygen as a tracer was injected into the downcomer of the

J-valve and an oxygen meter was utilized as the detector.

At first, the pressurized pure oxygen gas was input as a pulse from the tracer injection system which was set at 0.35 m from the top of the downcomer. The input pulse gas flowed downward through the void between the solid particles of the moving bed in the downcomer. Two oxygen meters (DO-236: TOA Co., Ltd.) as the detectors of C1 and C2 in Figure 1 were located at $L_1 = 0.30$ and $L_2 = 0.63$ m down from the tracer injection point on the downcomer. These oxygen sensor probes were inserted at the center from the side wall of the downcomer pipe. The signals of the oxygen concentration by each detector were measured with time. All data were automatically recorded using a computer.

Fig. 2(a) shows the time course of the oxygen concentration of the two detectors at C1 and C2 under typical conditions. Although the input signal was given as a pulse, the response has some distribution due to the diffusion of the oxygen gas. Therefore, the response signal became broader with the residence time of the tracer gas. The delaying time of the signals, t_G , was the difference between both peaks of the oxygen concentrations at C1 and C2. It was confirmed from pre-experiments that the delaying time t_G well corresponded to the averaged moving time of the gas bulk in the downcomer. Therefore, the superficial gas velocity in the downcomer U_{GD} was evaluated as follows.

$$U_{GD} = \left(\frac{L_2 - L_1}{t_G} \right) \varepsilon_{MF} \quad (1)$$

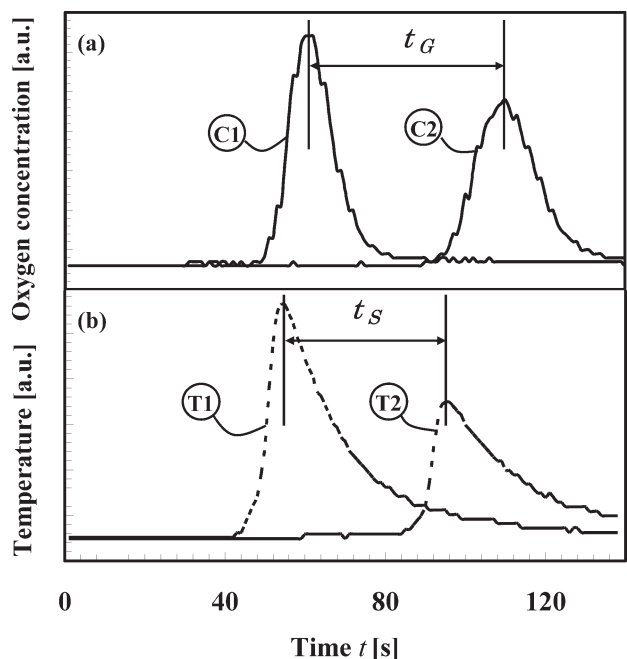


Fig. 2 – Simultaneous measurement of gas and solid streams using the tracer method

Measurement of solid stream in downcomer of J-valve

To simultaneously observe the solid particle stream through the J-valve, the hot particle tracer technique was used. A small amount of preheated solid particles were instantaneously injected using pressurized gas, which is identical to the oxygen gas tracer. The hot solid tracer flows with the bulk of the solid particles in the downcomer of the J-valve. Two digital thermometers (SK-L200T: SATO Co., Ltd.) as detectors of T1 and T2 in Figure 1 were located at $L_1 = 0.30$ and $L_2 = 0.63$ m, which are the same positions as C1 and C2. The thermo-sensors were inserted at the center of the cross section of the pipe as well as the oxygen sensor probes. The temperature at each detector was recorded with time.

Figure 2(b) shows the temperature changes of the two thermal detectors under typical conditions. The input thermal tracer's signal was given as a pulse as well as the gas tracer, the response signals were somewhat distributed due to the thermal diffusion. The response signal by the hot particle tracer also became broader with the residence time of the tracer. The delay between both peaks of each thermal detector at T1 and T2, t_s , means the time necessary to pass the distance $L_2 - L_1$. It was confirmed in the pre-experiment, that the necessary time, t_s , is equal to the superficial solid velocity in the downcomer. Under the fluidized conditions in this study, the solid particles in the downcomer never fluidize so that the voidage of the moving bed in the downcomer is the minimum fluidization velocity, ε_{MF} .

Therefore, the superficial solid velocity in the downcomer, U_s , was expressed as follows.

$$U_s = \left(\frac{L_2 - L_1}{t_s} \right) (1 - \varepsilon_{MF}) \quad (2)$$

Measurement of pressure difference in downcomer of J-valve

The digital differential pressure meter (DPG-502N: Okano Co., Ltd.) was used to measure the pressure drop in the downcomer of the J-valve. The higher pressure port of the pressure meter was connected at P6 in Figure 1 and the reference pressure port was connected at P7. The distance from P6 to P7 is $L_{ir} = 1.0$ m. In the section between P6 and P7, no entrance effect was observed and a stable and uniform moving bed was always formed under the experimental conditions in this study. Thus, the pressure drop, ΔP_{ir} , was evaluated from the differential pressure between P6 and P7.

The pressure drop in the downcomer, ΔP_{ir} , was simultaneously measured with the measurements of the gas and solid streams using the gas tracer and hot particle tracer. It was confirmed that ΔP_{ir} was

never influenced by the injection of the oxygen gas and hot solid particles.

The signals of the oxygen gas tracer concentration, hot particle tracer temperature and differential pressure were simultaneously recorded using a PC connected to a data-logger (NR-100: Keyence Co., Ltd.).

Measurement of pressure profiles in CFB

To understand the pressure balance in the entire CFB system, the pressure difference between each adjacent section was measured using pressure transducers (Model 239: Setra Systems Co., Ltd., DP-200 and DPG-502N: Okano Co., Ltd.) that were connected to every adjacent two ports of P1 to P10 in Figure 1. Namely, the pressure difference in the downcomer of the J-valve is described as ΔP_D which is the differential pressure at P8 for the pressure reference at P5. The pressure difference between P9 and P8 in the connector of the J-valve is ΔP_C . The pressure difference between P10 and P9 in the riser of the J-valve is ΔP_R . The pressure differences in the fast fluidized bed, the cyclone, the dipleg, the reservoir and the feeder were measured between each of adjacent pressure ports, that is, P2-P1, P3-P2, P4-P3, P5-P4 and P1-P10, which were expressed as ΔP_f , ΔP_{cyc} , ΔP_{dip} , ΔP_2 and ΔP_f , respectively.

All the pressure differences were recorded at all the inlet gas flow rates using a digital data processor (NR-100: Keyence Co., Ltd.).

Results and discussion

Superficial velocities of gas and solid in downcomer

The superficial solid velocity in the downcomer was simultaneously observed with the superficial gas velocity. Fig. 3 shows the relation between the superficial solid velocity, U_s , and the superficial gas velocity, U_{GD} , through the downcomer as a parameter of the pressure drop for the stable moving bed region in the downcomer, $\Delta P_{ir}/L_{ir}$. When the pressure drop in downcomer, $\Delta P_{ir}/L_{ir}$, was kept constant, U_s was quite proportional to U_{GD} . For a constant U_{GD} , U_s increased with the increasing $\Delta P_{ir}/L_{ir}$. The observed superficial solid velocity thus can be correlated as;

$$U_s \propto 1.28 U_{GD} \quad (3)$$

Therefore, the superficial solid velocity can be controlled by tuning the pressure difference in the downcomer and superficial gas velocity.

Pressure profile in CFB

Fig. 4 shows the pressure profiles in the CFB to the reference atmospheric pressure. The vertical

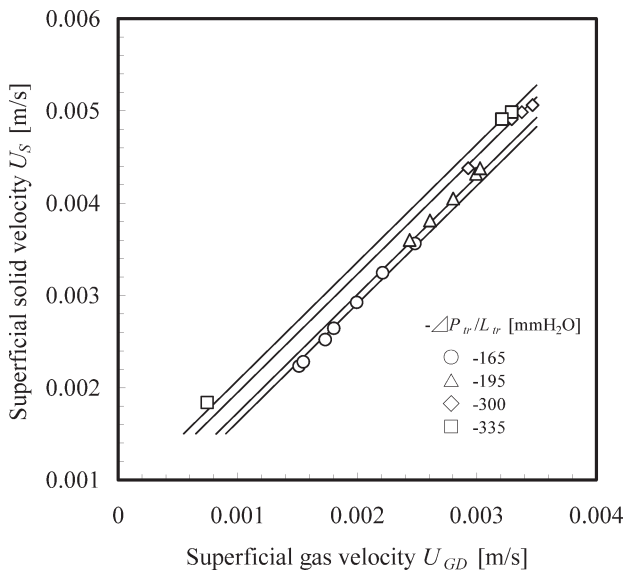


Fig. 3 – Effect of superficial gas velocity on superficial solid velocity

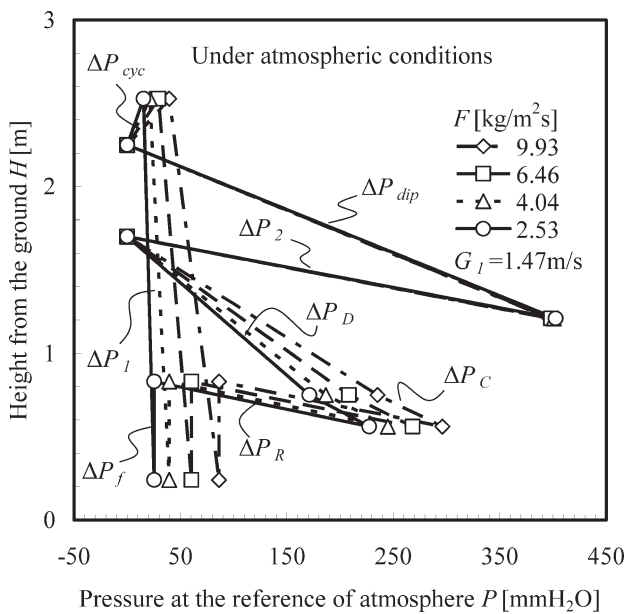


Fig. 4 – Pressure profile in CFB

axis is the height of the measuring points from the flower, H .

When the circulating mass flux of solid F was changed from 2.53 kg/(m²·s) to 9.93 kg/(m²·s), the pressure profiles were experimentally observed.

The pressure differences in the dipleg ΔP_{dip} , the reservoir ΔP_2 , the riser ΔP_R and the feeder ΔP_f hardly depend on the circulating mass flux of the solid F . On the other hand, the pressure difference in the J-valve, $\Delta P_D + \Delta P_C + \Delta P_R$ depended more significantly on F than the other pressure differences. Therefore, it is important to evaluate the pressure profile in the J-valve to control the solid circulation rate in the CFB.

Pressure profiles in J-valve

To discuss in more detail the mixed flow of air and solid particles in the J-valve, the pressure profile in the J-valve was redrawn in Fig. 5. The pressure profiles were described along the particle flow route at the references to the pressure and the position at the top end of the downcomer.

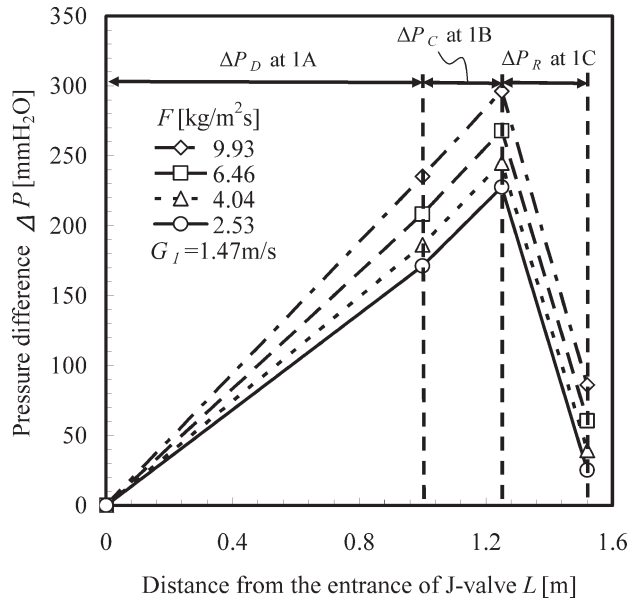


Fig. 5 – Pressure profile in J-valve

It was observed that only the pressure gradient in the downcomer, ΔP_D , increased with the increasing circulating mass flux of the solid F . Therefore, the pressure difference in the downcomer, ΔP_D , very strongly influenced F , and vice versa. On the other hand, the changes in the pressure gradients in the connector and the riser, ΔP_C and ΔP_R , did not significantly change F . Thus, the pressure control in the downcomer was the most important factor for controlling the circulation rate of the solid particles in the CFB.

Pressure balance between superficial solid velocity and superficial gas velocity in the downcomer

Terasaka *et al.*¹⁸ proposed a relative superficial gas velocity to take into account the solid particle flow in order to understand the behavior of a moving bed flow. It was applied to the present system in the downcomer of the J-valve. Almost all of the pressure drop in the downcomer was derived from the friction loss of gas through the void in the bed so that the relative superficial gas velocities in the downcomer, ΔU_{GD} , was defined as;

$$\Delta U_{GD} = U_{GD} - \frac{\varepsilon_{MF}}{1 - \varepsilon_{MF}} U_S \quad (4)$$

where U_S is the superficial solid velocity. U_{GD} and ϵ_{MF} are the superficial gas velocities in the downcomer and the fractional voidage at the minimum fluidization state, respectively.

Fig. 6 shows the pressure drops between the two pressure ports in the downcomer, $\Delta P_{tr}/L_{tr}$. The pressure drop, $\Delta P_{tr}/L_{tr}$ was plotted with the relative superficial gas velocity with respect to the particle velocity in the downcomer, ΔU_{GD} , for all of the experimental results. The pressure drop in the downcomer, $-\Delta P_{tr}/L_{tr}$, increased with the increasing ΔU_{GD} although the experimental data were slightly scattered due to turbulence caused by the inserted probes.

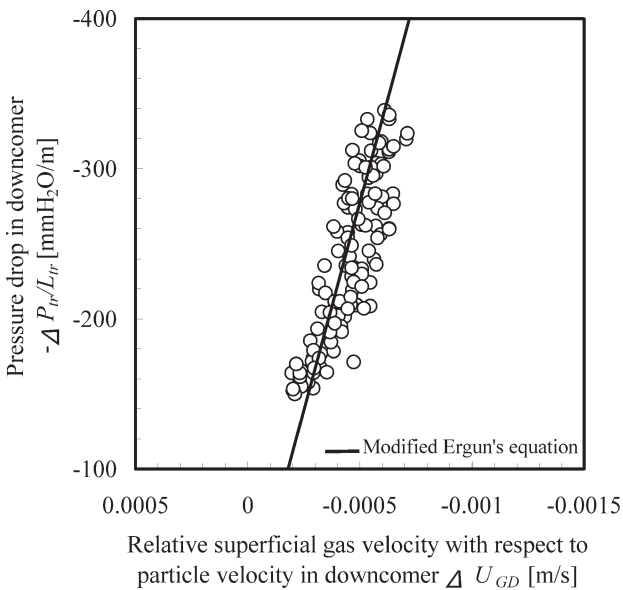


Fig. 6 – Relation between pressure drop and relative superficial gas velocity in downcomer

Terasaka *et al.*¹⁸ investigated using an *isolated* J-valve to explain the relation between the pressure drop and the superficial gas velocity for the moving bed in the downcomer. By analyzing the experimental results, the modified Ergun's equation in which the superficial gas velocity was replaced by the relative superficial gas velocity to the solid flow velocity was proposed as follows:

$$-\frac{\Delta P_D}{L_D} = 150 \frac{(1 - \epsilon_m)^2}{\epsilon_m^3} \frac{\mu \Delta U_{GD}}{(\phi d_p)^2} + 1.75 \frac{1 - \epsilon_m}{\epsilon_m^3} \frac{\rho_G |\Delta U_{GD}| \Delta U_{GD}}{\phi d_p} \tag{5}$$

where ϵ_m is the fractional voidage in the moving bed. Although the equation well estimated the relation between the pressure drop in the downcomer and the relative superficial gas velocity in the downcomer of the isolated J-valve, it has not yet

been confirmed at the J-valve mounted in the CFB in spite of the industrial importance.

Therefore, in this study the pressure drop in the downcomer calculated using modified Ergun's equation, Eq. (5), was compared with the experimental pressure drop in the downcomer. The estimated pressure drop, which is drawn as a line in Figure 6, agreed well with the experimental results which are obtained at the J-valve set in the CFB. Therefore, the presented equation can be used for designing of not only an isolated J-valve, but also a J-valve in CFB system.

Estimation of superficial solid velocity in the downcomer

It is important for the design of CFBs to estimate the superficial solid velocity because the solid flow rate through a J-valve corresponds to the circulating flow rate of the solid particle. Under the operating conditions in this study, it can be considered that the gas stream in the downcomer forms a laminar flow. Thus, the second term on the right hand side of modified Ergun's equation shown in Eq. (5) is negligible so that it was rearranged as follows:

$$U_S = \frac{1 - \epsilon_m}{\epsilon_m} U_{GD} + \frac{1}{150} \frac{\Delta P_D}{L_D} \frac{\epsilon_m^2}{(1 - \epsilon_m)} \frac{(\phi d_p)^2}{\mu} \tag{6}$$

When $\epsilon_m \approx \epsilon_{MF}$ the factor of U_{GD} can be calculated.

$$U_S \propto 1.278 U_{GD} \tag{7}$$

Equation (7) agreed well with Equation (3). Namely, the superficial solid velocity, U_S , can be linearly controlled using the superficial gas velocity in the downcomer of the J-valve, U_{GD} .

Fig. 7 shows the comparison between the experimental results and the calculated superficial solid

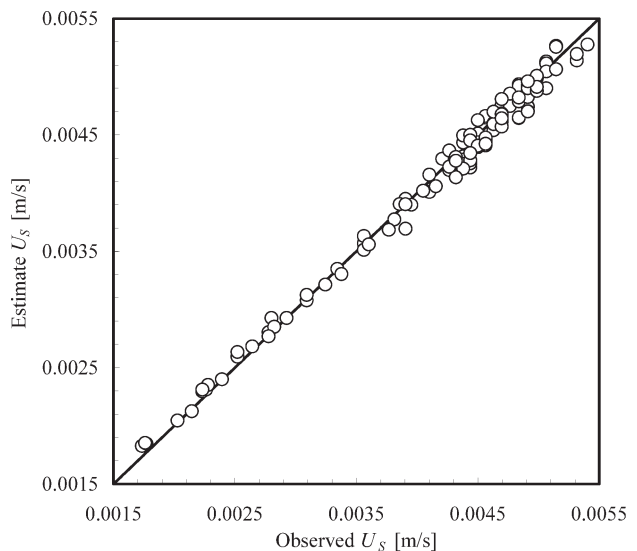


Fig. 7 – Estimation of superficial solid velocity

velocity using Eq. (7). The prediction sufficiently agreed with the experimental superficial solid velocity so that the proposed equation is valid for estimating and controlling the solid flow in the CFB.

Conclusions

To experimentally monitor the gas and solid streams in the downcomer of a J-valve as a pneumatic solid feed device mounted in the CFB, a simultaneous measurement technique using the oxygen gas tracer and the hot particle tracer with the pressure transducers was developed. The novel measurement technique was reliable and available for observing gas-solid flow in a moving bed in real-time. By using this measurement technique, the dependence of the solid flow on the gas flow in the moving bed in the downcomer of J-valve was clarified.

The pressure profile and the pressure balance in a CFB containing a J-valve were investigated. It was found that the circulating mass flux in a CFB or solid flow in a J-valve was significantly governed by the pressure drop in the downcomer of the J-valve.

By correlating the superficial gas velocity, the superficial solid velocity and the pressure drop in the downcomer obtained by simultaneous measurements, it was clarified that the pressure drop in the downcomer was well estimated even in the J-valve set in a CFB using modified Ergun's equation. Therefore, the solid circulation rate in a CFB can be predicted by monitoring the pressure drop and superficial gas velocity in the downcomer of the J-valve.

To quantitatively control the circulating rate of the solid particles in the CFB, monitoring and optimizing the superficial gas velocity in the downcomer of the J-valve are important.

ACKNOWLEDGEMENT

The authors are indebted to the Kaneka Corporation for support of this research.

Nomenclature

| | |
|------------|---|
| d_p | – particle diameter [m] |
| F | – mass flux or circulating mass flux of solid particles [$\text{kg}/(\text{m}^2 \cdot \text{s})$] |
| G | – volumetric gas flow rate [m^3/s] |
| H | – height from the ground [m] |
| L | – length [m] |
| ΔP | – pressure drop [Pa] |
| U_G | – superficial gas velocity [m/s] |
| U_S | – superficial solid velocity [m/s] |

| | |
|--------------|---|
| ΔU_G | – relative superficial gas velocity with respect to particle velocity [m/s] |
| U_{MF} | – minimum fluidization velocity [m/s] |
| U_S | – superficial particle velocity [m/s] |

Greek

| | |
|--------------------|--|
| ε_{MF} | – fractional voidage in minimum fluidization state [–] |
| ε_m | – fractional voidage in moving bed [–] |
| μ | – gas viscosity [$\text{Pa} \cdot \text{s}$] |
| ρ_g | – gas density [kg/m^3] |
| ρ_s | – particle density [kg/m^3] |
| ϕ | – sphericity [–] |

Literature cited

1. Van de Velden, M. Baeyens, J., *Chem. Eng. Sci.* **62** (2007) 2139–2153.
2. Lei, H., Horio, M., A, J. *Chem. Eng. Japan* **31** (1998) 83–94.
3. Kim, S. W., Kim, S. D., Lee, D. H., *Ind. Eng. Chem. Res.* **41** (2002) 4949–4956.
4. Rhodes, M. J., Geldart, D., *Powder Technol.* **53** (1987) 155–162.
5. Basu, P., Cheng, L., *Chem. Eng. Res. Des.* **78** (2000) 991–998.
6. Smolders, K., Baeyens, J., *Powder Technol.* **119** (2001) 269–291.
7. Gupta, S. K., Berruti, F., *Powder Technol.* **108** (2000) 21–31.
8. Horio, M., Mori, S., *Fluidization Handbook*, APPIE, Baifu-kan, Japan, 1999.
9. Mori, S., Yan, Y., Kato, K., Matubara, K., Liu, D., *Hydrodynamics of Circulating Fluidized Bed*, in Basu, P., Horio, M., Hasatani, M., (Eds.), *Circulating Fluidized Bed Technology III*, 113–118, Oxford, England, 1991.
10. Oshima, H., Wachi, S., Terasaka, K., *Bul. Japanese Pat. Inst.* (1993) H5-262680.
11. Wachi, S., Oshima, H., Terasaka, K., *Eur. Pat. Appl.*, (1993) EP 521382A2.
12. Yoon, S. M., Kunii, D., *Ind. Eng. Chem. Proc. Des. Dev.*, **9** (1970) 559–565.
13. Daous, M. A., Al-Zahrani, A. A., *Powder Technol.* **99** (1998) 86–89.
14. Kunii, D., Levenspiel, O., *Fluidization Engineering*, 2nd Ed., Butterworth-Heinemann, USA (1991).
15. Geldart, D., Jones, P., *Powder Technol.* **67** (1991) 163–174.
16. Yang, W. C., Knowlton, T. M., *Powder Technol.* **77** (1993) 49–54.
17. Kim, S. W., Namkung, W., Kim S. D., *Chem. Eng. Technol.* **24** (2001) 843–849.
18. Terasaka K., Akashi, S., Tsuge, H., *Powder Technol.* **126** (2002) 13–21.
19. Kojima, T., Ishihara, K., Guilin, Y., Furusawa, T., *J. Chem. Eng. Japan* **22** (1989) 341–346.
20. Smolders, K., Baeyens, J., *Chem. Eng. Sci.* **55** (2000) 4104–4116.
21. Bhusarapu, S., Al-Dahhan, M. H., Dudukovic, M. P., *Chem. Eng. Sci.* **59** (2004) 5381–5386.
22. Gayan, P., Deigo, L.F. de, Adanez, J., *Powder Technol.* **94** (1997) 163–171.
23. Li, Y., Lu, Y., Wang, F., Han, K., Mi, W., Chen, X., Wang, P., *Powder Technol.* **91** (1997) 11–16.

